# Adenosine-Derived Inhibitors of 78 kDa Glucose Regulated Protein (Grp78) ATPase: Insights into Isoform Selectivity[†]

Alba T. Macias,* Douglas S. Williamson, Nicola Allen, Jenifer Borgognoni, Alexandra Clay, Zoe Daniels, Pawel Dokurno, Martin J. Drysdale, Geraint L. Francis, Christopher J. Graham, Rob Howes, Natalia Matassova, James B. Murray, Rachel Parsons, Terry Shaw, Allan E. Surgenor, Lindsey Terry, Yikang Wang, Mike Wood, and Andrew J. Massey

Vernalis (R&D) Ltd., Granta Park, Great Abington, Cambridge, CB21 6GB, U.K.

Ⓢ *Supporting Information*

ABSTRACT: 78 kDa glucose-regulated protein (Grp78) is a heat shock protein (HSP) involved in protein folding that plays a role in cancer cell proliferation. Binding of adenosine-derived inhibitors to Grp78 was characterized by surface plasmon resonance and isothermal titration calorimetry. The most potent compounds were **13** (VER-155008) with $K_D = 80$ nM and **14** with $K_D = 60$ nM. X-ray crystal structures of Grp78 bound to ATP, ADPnP, and adenosine derivative **10** revealed differences in the binding site between Grp78 and homologous proteins.
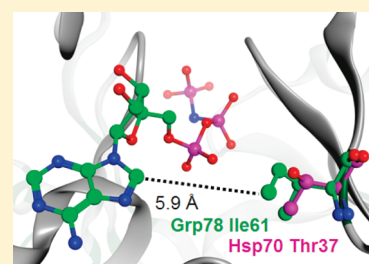
INTRODUCTION

The Hsp70 family of molecular chaperones represents one of the most evolutionarily conserved groups of chaperone proteins involved in protein folding.[1,2] Hsp70 proteins have an N-terminal ATPase and a C-terminal substrate binding domain (SBD) connected via a linker.[3] The binding and release of peptide substrates in the SBD are coupled to ATP hydrolysis, which causes conformational changes in the protein.[4] The ATP-bound state has low substrate affinity, and the ADP-bound state has high substrate affinity. Cochaperone proteins such as J domains stimulate ATP hydrolysis,[5] while nucleotide exchange factors such as Bag-1[6] enhance ATPase activity by facilitating ADP release.

Glucose regulated protein 78 (Grp78), also known as BiP or HSP5A, is the Hsp70 isoform located predominantly in the endoplasmic reticulum (ER),[7] while Hsp70 and Hsc70 isoforms are located in the cytosol. As a key component of the ER chaperoning function, Grp78 ensures proper protein folding, preventing aggregation and targeting misfolded proteins for degradation within the ER as well as binding calcium and regulating ER stress signaling.[8]

Grp78 has been shown to play a role in tumor proliferation, survival, and angiogenesis.[9,10] Grp78 overexpression in tumor cells appears necessary to survive oncogenic stress. Elevated glucose metabolism leads to glucose starvation, low pH, and severe hypoxia, which are conditions under which cancer cells must survive, and are all factors that induce ER stress and activation of the Grp78 promoter. Grp78 has also been found on the cell membrane of cancer cells,[11,12] where it has been shown to interact with proteins involved in oncogenic signaling.[13,14] Grp78 overexpression also provides resistance to chemotherapeutic agents in multiple tumor cell lines.[15,16] Therefore, inhibiting Grp78

expression or its pharmacological activity could have important therapeutic benefits in the fight against cancer.

Known inhibitors targeting Grp78 activity or its induction are derived from natural products. Genistein and (−)-epigallocatechin gallate (EGCG) inhibit the pharmacological activity of Grp78, while the bacterial AB5 subtilase cytotoxin specifically cleaves Grp78 at a single amino acid.[17] These agents were able to selectively inhibit the growth of cancer cells or sensitize them to cytotoxic chemotherapy. Genistein and EGCG act on many cellular pathways and components in addition to Grp78. The macrocycle versipelostatin (VST) inhibits the transcriptional activation of the unfolded protein response (UPR) target genes Grp78 and Grp94 and inhibited MNK047 tumor xenograft growth.[18] Grp78 can also be found in the cell membranes of cancer cells, and recent therapeutic approaches have targeted the membrane-bound SBD. A prodrug that contains a cyclic 13-mer peptide (Pep42) was shown to bind to Grp78 and was internalized into the cell.[19,20] Antibodies that bind to the SBD inhibited cell proliferation and induced apoptosis in prostate cancer cells and melanoma cells.[21]

Interest in Grp78 as an oncology target, the lack of structural data on inhibitors binding to the ATPase domain, and the unexplored questions of isomer selectivity prompted the current study. In-house studies comparing the effect of siRNA knockdown of Hsp70, Hsc70, and Grp78 corroborate the role of Grp78 in cell proliferation. We recently reported potent and novel nucleoside inhibitors for the ATPase domain of the Hsp70/Hsc70 isoforms. Compounds from our Hsp70 program[22,23]

Scheme 1[a]

a; R= Ph
b; R= cyclohexyl
c; R = 3-pyridyl
d; R= carboxamide
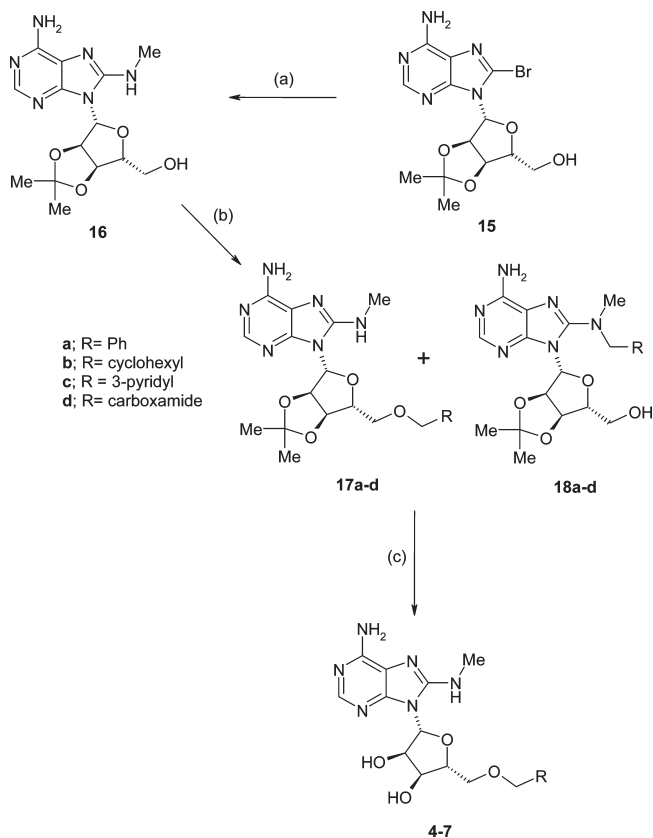
[a] Reagents and conditions: (a) MeNH$_2$, EtOH, 130 °C, microwave, 91%; (b) Cs$_2$CO$_3$, RCH$_2$Cl, DMF, 40−50%; (c) CF$_3$CO$_3$H, 18−25%.

Scheme 2[a]
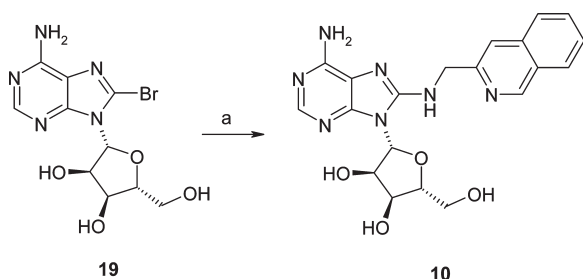
[a] Reagents and conditions: (a) 1-(isoquinolin-3-yl)methanamine, EtOH, 170 °C, microwave, PS-benzaldehyde, 25%.

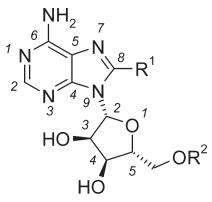**Table 1. Binding Data for Inhibitors with Grp78 and Hsp70**
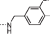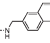
	R^1	R^2	Grp78 SPR K_D (μM)[a]	Grp78 SPR k_d (s^{-1})[a]	Hsp70 FP K_i (μM)[a]	Hsp70 SPR K_D (μM)[a]
1	H		2.17	0.005	0.11[b]	0.5
2	NH$_2$	H	6.80	>1	4.46	11
3	NHMe	H	7.46	>1	8.3	-
4	NHMe		0.99	>1	1.1	-
5	NHMe		4.36	>1	4.07	-
6	NHMe		2.71	>1	0.45	-
7	NHMe		12.36	>1	1.85	-
8		H	0.99	0.5	4.31	-
9		H	0.23	0.2	1.29	-
10		H	2.41	0.4	4.32	-
11		Me	0.25	0.4	1.44	-
12			0.77	0.3	1.05	-
13			0.08	0.09	0.12[b]	0.3
14			0.06	0.04	0.31[b]	0.05

[a] All IC$_{50}$, K_D, and GI$_{50}$ are the mean of at least two determinations.
[b] Value at the detection limit in the FP assay.

enabled us to study Grp78 inhibition and isomer selectivity. Inhibitor binding was studied by surface plasmon resonance (SPR) and isothermal titration calorimetry (ITC). We report the first X-ray crystallographic structures of the ATPase domain of apo Grp78 and in complex with adenosine 5′-triphosphate (ATP), 5′-adenylyl β,γ-imidodiphosphate (ADPnP), and a nucleoside inhibitor. The modest selectivity seen in the binding data for Grp78 and Hsp70 is discussed in the context of structure.

■ **RESULTS**

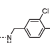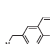**Inhibitor Synthesis.** The syntheses of 2,[24] 3,[25] 8, 9, and 11−14[22] have been previously reported. Compounds 4−7 were synthesized as shown in Scheme 1. Treatment of 8-bromo-2′-3′-O-(1-methylethylidene)adenosine 15[26] with methylamine afforded the 8-methylamino derivative 16.[27] Reaction of compound 16 with a range of primary alkyl chlorides in the presence of cesium carbonate afforded intermediates 17a−d and 18a−d as inseparable mixtures. Further treatment of this mixture with trifluoroacetic acid resulted in removal of the acetonide protecting group and decomposition of the undesired regioisomers 18a−d, enabling isolation of 4−7 in 18−25% yield. Compound 10 was synthesized using existing methodology[22,28] by treatment of 8-bromoadenosine 19 with 1-(isoquinolin-3-yl)methanamine (Scheme 2).

Table 2. Thermodynamic Binding Data and Cell Assay Results

	R^1	R^2	Grp78 SPR K_D (μM)[a]	Grp78 ITC K_D (μM)[a,b]	Grp78 ITC ΔH (kcal/mol)[a]	Grp78 ITC ΔS (cal/mol/°)[a]	HCT116 GI$_{50}$ (μM)[a,c]
1	H	(phosphate group)	2.17	3.83[d]	-1.3[d]	20.4[d]	-
2	NH$_2$	H	6.80	14.14[d]	-13.2[d]	-22.0[d]	0.05[e]
8	(dichlorobenzyl amino)	H	0.99	0.87	-12.4	-13.6	26
9	(quinoline amino)	H	0.23	0.35	-18.2	-31.5	>80
13	(dichlorobenzyl amino)	(cyanophenyl)	0.08	0.20	-15.1	-11.2	5
14	(quinoline amino)	(cyanophenyl)	0.06	0.10	-17.5	-26.7	>80

[a] All ITC and GI$_{50}$ are the mean of at least two determinations unless otherwise stated. [b] ITC $K_D = 1/K_A$. [c] Reference 22. [d] $n = 1$ [e] Low GI$_{50}$ due to predominantly non-HSP70 mechanism.

Inhibitor Binding Studies. Binding of compounds to Grp78 (Table 1) was assessed using SPR to measure the dissociation constant (K_D) and off-rates (k_d). Adenosine 5′-diphosphate (ADP, **1**) had the slowest off rate ($k_d = 0.005\ \text{s}^{-1}$) but not the smallest K_D (2.17 μM). Compounds **2** and **3** contain an 8-amino and 8-methylamino substituent on the adenine core and have similar K_D of 6.80 and 7.46 μM, indicating that the additional methyl has little effect on binding affinity. When binding to the Hsp70 isoform, the 8-amino group in **2** resulted in 60-fold improvement over the hydrogen in adenosine, likely due to an internal hydrogen bond.[22]

Compounds **4**−**7** explore the effect of substituents at the R^2 position when R^1 is 8-methylamino. Changing the phenyl in **4** ($K_D = 0.99\ \mu$M) to an amide in **7** ($K_D = 12.36\ \mu$M) resulted in a 12-fold loss of binding affinity in Grp78. Compounds **8**−**10** explore aromatics substituents in R^1, keeping R^2 as hydrogen. The quinoline in **9** provided affinity gains of 4-fold and 10-fold compared to aromatics in **8** and **10**. Aromatic substituents at R^1 in **8**−**10** result in slower off-rates ($k_d = 0.2−0.5\ \text{s}^{-1}$) than those observed for compounds **4**−**7** ($k_d > 1\ \text{s}^{-1}$), even for compounds with similar K_D. Changing the hydrogen in **8** to a methyl (**11**) improved affinity by 4-fold. Compounds **12**−**14** have aryl substituents in R^1 and R^2. Comparing **12** and **13** reveals that the addition of a nitrile increases affinity by 10-fold.

To allow relative comparisons between Grp78 and Hsp70 affinities, K_i values for Hsp70 were calculated from the FP IC$_{50}$ using equations assuming a tight inhibitor and free concentrations.[29,30] For the more potent inhibitors, SPR was used to measure K_D, since the Hsp70 FP assay used a protein concentration of 400 nM, which means that the assay response is limited to compounds with affinities greater than 300 nM. The values and
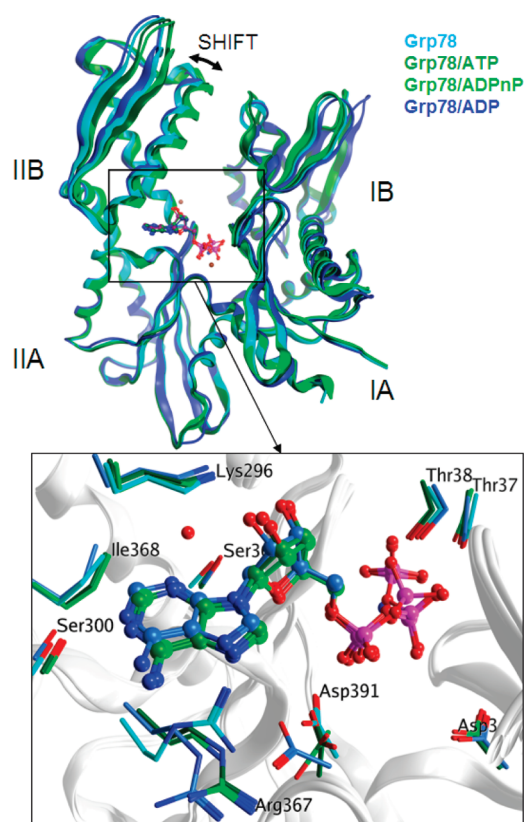

Figure 1. X-ray crystallography structures of Grp78/Apo (cyan, 3LDN), Grp78/ADPnP (green, 3LDO), and Grp78/ATP (3LDL) are shown superimposed with Grp78/ADP[31] (blue, 3IUC). Detail of the binding site shows residue positions near ligands.

rank ordering for compounds **2**−**5** are similar in Grp78 and Hsp70. However, changing the phenyl in **4** to more polar substituents (pyridyl **6**, primary carboxamide **7**) lowers binding in Grp78 but has little effect on Hsp70 binding. Binding of **7** is 12-fold lower than binding of **4** in Grp78 but only change by 2-fold in Hsp70. The addition of aromatic subsituents in R^1 (**8**−**11**), compared to **2** and **3**, increases potency more significantly in Grp78 than Hsp70.

Binding was confirmed for several compounds by ITC from which the dissociation constant and enthalpic and entropic contributions were obtained (K_D, ΔH, ΔS) as reported in Table 2. K_D values obtained with ITC were usually within 2-fold of those obtained with SPR. The quinoline (**9** and **14**) provides an enthalpic gain over the dichloro substituent (**8** and **13**), which is balanced by a decrease in entropy loss resulting in only small improvements in overall K_D. Despite the quinoline's higher affinity for the protein shown by quinolines **9** and **14**, they did not inhibit cell growth like the less potent dichloro compounds.

Structure of Grp78 Bound to ADPnP and ATP. Structures of the crystallized Grp78 ATPase domain (residues 24−407) in the apo form and with soaked ligands were solved by X-ray crystallography. Figure 1 illustrates that there are no large conformational changes upon binding of ADPnP and ATP, which caused the Cα backbone RMSDs to change by only 0.67 and 0.54 Å, respectively. The main change is the shift observed in domain IIB. Comparison with the cocrystal of Grp78/ADP solved by Wisniewska and co-workers (3IUC), which crystallized with a different space group and packing,[31] shows a very similar binding
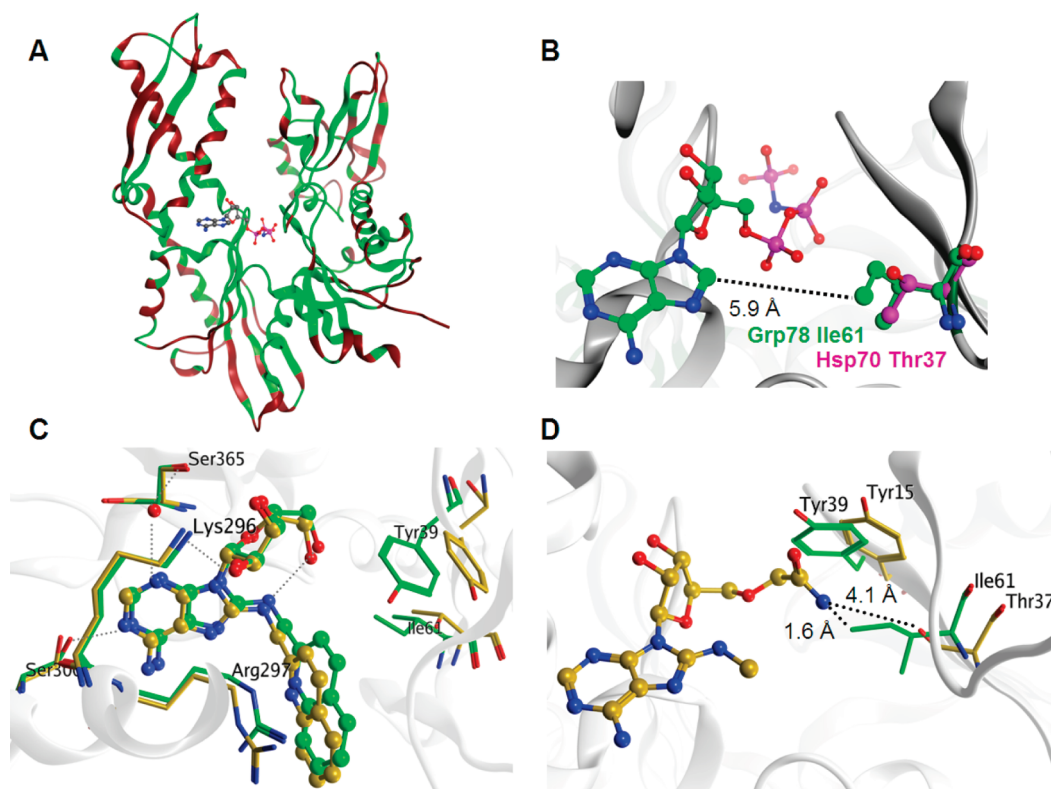
Figure 2. (A) Conserved residues among Hsp70 isoforms (Grp78, Hsp70, Hsc70, Hsp70B′, Hsp701-Hom, Hsp70-2) are shown in green on the ribbon representation of the Grp78/ADPnP structure; nonconserved residues are in red. (B) Within 4.5 Å around ADPnP, only one residue differs between Grp78 and Hsp70 in the binding site. (C) Overlay of X-ray crystal structures of **10** bound to Grp78 and Hsc70/Bag reveals similar binding mode for inhibitor. (D) Crystal structure of Hsc70/Bag-1 with **7** reveals that the amide π-stacks with Tyr15 and interacts with Thr37 through a water mediated H-bond. Overlay with apo Grp78 shows that the polar amide would be too close to the hydrophobic Ile61 in Grp78.

site. The Cα backbone rmsd values of 0.74 and 0.95 Å between Grp78/ADP and our Grp78 and Grp78/ATP structures are mostly due to surface residues.

Comparison of Grp78, Hsp70, and Hsc70 Structures. Grp78 is the least conserved isoform within the Hsp70 family members. The closest homologue of Grp78 based on ATPase sequence is Hsc70 with 70% residue identity as analyzed with BLAST,[32] while the residue identity between Hsc70 and Hsp70 is 89%. Sequence alignments can be found in Supporting Information. Figure 2A highlights the residues that differ between Grp78 ATPase and other Hsp70 isoforms. The ATPase structures[31] of these isoforms showed that they have the same secondary fold and a highly conserved binding site, with most differences in residues located at the protein surface.

Comparison of the X-ray crystallographic structures of Grp78 and Hsp70 (Figure 2B) showed that there is one residue that is different within a radius of 4.5 Å around ADPnP. Grp78 has an isoleucine (Ile61) where Hsp70 has a threonine (Thr37). The remaining binding site residues are conserved and have similar conformations except for the solvent exposed Arg297, Arg367, and Glu293 which occupy slightly different positions in some of the structures.

Structures of Inhibitors Bound to Grp78 and Hsc70/Bag-1. Superimposition of the X-ray crystallography structures of **10** bound to Grp78 and Hsc70/Bag-1 in Figure 2C shows a similar binding mode in Grp78 and Hsc70/Bag-1. While **10** is not one of the more potent compounds, it was one for which we had obtained crystals in both proteins. Crystals of Hsc70 were used

as a surrogate for Hsp70, since they were more amenable to crystallography and there is high homology between Hsp70 and Hsc70. Hsc70 was crystallized in complex with its cochaperone Bag-1, which opens up the ATPase domain by separating domains IB and IIB. The presence of Bag-1 results in a larger binding cavity reflected in the increased distance between the residues in domain IB (Tyr and Ile) and residues in domain IIB which bind the adenine. Several attempts to soak in the potent diaryl inhibitors into the closed forms of Hsp70 and Grp78 failed. A homology model of an open conformation of Grp78, built using the Hsc70/Bag-1/**14** structure (3fzm)[22] as template, suggests that **14** could bind in a similar mode as it does in Hsc70/Bag-1 (Figure S3 in Supporting Information).

Figure 2D illustrates the location of the amide substituent of **7** bound to Hsc70/Bag-1. In Hsc70, the amide π-stacks with Tyr15 and interacts with Thr37 via bridging water molecules. Superimposing the complex of Hsc70/Bag-1/**7** with a structure of Grp78 shows that the polar amide in **7** would be in proximity to the hydrophobic residue Ile61, which should be detrimental to potency.

■ DISCUSSION AND CONCLUSIONS

We have studied the inhibition of Grp78 due to its potential interest as an oncology target. In-house studies comparing the effect of siRNA knockdown of Hsp70, Hsc70, and Grp78 corroborate the role of Grp78 in cell proliferation. siRNA knockdown of Grp78 had a greater effect on tumor cell growth than knockdown of the cytosolic Hsp70 or Hsc70 in a panel of 10

human cancer cells (Figure S2 in Supporting Information). Binding of compounds to Grp78 was investigated by SPR, ITC, and X-ray crystallography. SPR and ITC produced highly correlated K_D, providing additional information on the off-rates and thermodynamic energy terms. The slow off-rate of ADP (**1**) (k_d = 0.005 s^{-1}) is consistent with the need for nuclear exchange cofactor proteins to help release ADP from the binding site of Hsp70 proteins. The nucleoside inhibitors tested in ITC showed a high enthalpic contribution which was counterbalanced by disfavorable entropic contribution. The quinoline containing ligands **9** and **14** were slightly more potent, had better enthalpic contributions, and slower off-rates than the dichlorophenyl inhibitors **8** and **13**. However, previously published data obtained for HCT116 cells indicated that only the dichloro compounds were able to stop cell growth in cell-based assays,[22] likely due to physicochemical properties affecting the ability of the compounds to reach the target protein.

The most potent compound with cellular activity, VER-155008 (**13**, HCT116 GI$_{50}$ = 5 μM), has similar potencies in both Grp78 and Hsp70, thus this compound is likely a nonselective pan-inhibitor for similar protein isoforms of the Hsp70 family. Crystal structures of Hsp70 and Grp78 reveal that while most residues are conserved within the binding site, one residue differs between Grp78 and Hsp70 and has the potential to be used for designing in selectivity between Grp78 and the other Hsp70 isoforms. Selectivity between Hsp70 and Grp78 was observed for two compounds (**6**, **7**) that contained polar substituents in R^2. The change from a polar Thr37 in Hsp70 to nonpolar Ile61 in Grp78 creates a more hydrophobic binding site in Grp78 which could explain why polar substitutents at the R^2 position were more detrimental to affinity in Grp78 than Hsp70. The increased hydrophobicity in Grp78 could be exploited in ligand design to achieve further potency; our library of nucleoside inhibitors was initially designed for Hsp70 and contained few hydrophobic and saturated substituents in R^2. Nevertheless, the polarity, size and flexibility of the overall ATP binding pocket still pose a challenge to achieve high affinity binding by small druglike molecules.

Using a combination of surface plasmon resonance and isothermal titration calorimetry, we have identified submicromolar inhibitors of Grp78 that bind to the ATPase domain of this molecular chaperone. X-ray crystallographic studies of a nucleoside inhibitor bound to Grp78 revealed key structural differences between Grp78 and the closely homologous proteins Hsc70 and Hsp70. This has allowed us to rationalize the modest selectivity for Grp78 observed in certain nucleoside analogues. These molecules, which to our knowledge are the first inhibitors known to bind to the ATPase domain of Grp78, may serve as useful chemical tools to further probe the biology of Grp78.

■ EXPERIMENTAL SECTION

General Methods. All commercial reagents were used without further purification. Anhydrous solvents were obtained from commercial sources and used without further drying. Flash chromatography was performed with prepacked silica gel cartridges (IST Flash II, 54 Å, Biotage Ltd., Hengoed, U.K.). Thin layer chromatography was conducted with 5 cm × 10 cm plates coated with Merck Type 60 F$_{254}$ silica gel. Microwave heating was performed with a Biotage Initiator 2.0 instrument.

Compound purity was assigned by liquid chromatography—mass spectrometry (LC—MS) at pH 4; all compounds had ≥95% purity.

LC—MS was performed using a Hewlett-Packard 1100 series instrument linked to a quadrupole detector. The column was a Phenomenex Luna 3 μm C18(2), 30 mm × 4.6 mm i.d. Buffer A was prepared by dissolving 1.93 g of ammonium acetate in 2.5 L of HPLC grade water and adding 2 mL of formic acid. Buffer B was prepared by adding 132 mL of buffer A to 2.5 L of HPLC grade acetonitrile and adding 2 mL of formic acid. The elution gradient was buffer A—buffer B (95:5 to 5:95) over 3.75 min. Flow rate was 2.0 mL min^{-1}. Retention times (t_R) are reported in minutes. Ionization is positive, unless otherwise stated. Nuclear magnetic resonance (NMR) analysis was performed with a Bruker DPX400 spectrometer, and proton NMR spectra were measured at 400 MHz. The spectral reference was the known chemical shift of the solvent. Proton NMR data are reported as follows: chemical shift (δ) in ppm, followed by the integration, the multiplicity (s = singlet, d = doublet, t = triplet, q = quartet, p = pentet, m = multiplet, dd = doublet of doublets, and br = broad), and the coupling constant rounded to the nearest 0.1 Hz.

Compound **4** was purified by preparative HPLC at pH 4, performed on a Waters FractionLynx MS autopurification system, with a Gemini 5 μm C18(2), 100 mm × 20 mm i.d. column from Phenomenex, running at a flow rate of 20 mL min^{-1} with UV diode array detection (210—400 nm) and mass-directed collection. Solvent A was 10 mM ammonium acetate in HPLC grade water + 0.08% v/v formic acid. Solvent B was 95% v/v HPLC grade acetonitrile + 5% v/v solvent A + 0.08% v/v formic acid. The gradient was (time, % solvent B) 0 min, 5%; 1 min, 8%; 7 min, 28%; 7.5 min, 95%; 9.5 min, 95%; 10 min, 5%. The mass spectrometer was a Waters Micromass ZQ2000 instrument, operating in positive or negative ion electrospray ionization modes, with a molecular weight scan range of 150—1000. IUPAC chemical names were generated using AutoNom Standard.

Compounds **1** (Sigma-Aldrich Ltd.) and **2** (Toronto Research Chemicals) are commercially available, and **3**,[25] **8**, **9**, and **11**—**14**,[22] and **15**[26] have been previously described. Compounds **4**—**7** were prepared as shown in Scheme 1; **10** was prepared as shown in Scheme 2.

(2R,3R,4S,5R)-2-(6-Amino-8-methylaminopurin-9-yl)-5-benzyloxymethyltetrahydrofuran-3,4-diol (4). A solution of **17a** and **18a** (0.044 g, 0.10 mmol) in trifluoroacetic acid (2 mL) was stirred at room temperature overnight. The solvent was then removed in vacuo followed by repeat coevaporation with methanol. The resulting crude product was purified by preparative LC—MS at pH 4, which afforded a clear glass, identified as **4** (0.007 g, 0.019 mmol, 18%). LC—MS: m/z 387 [M + H]$^+$; t_R = 1.64 min; total run time 3.75 min. ^{1}H NMR: δ_H (DMSO-d_6) 7.89 (1 H, s, Ar-H), 7.35 (5 H, m, Ph), 6.50 (2 H, s, NH$_2$), 6.41 (1 H, q, J 4.6 Hz, MeNH), 5.81 (1 H, d, J 6.2 Hz, 2-H), 5.35 (1 H, br s, 3-OH), 5.25 (1 H, br s, 4-OH), 4.76 (1 H, t, J 5.9 Hz, 3-H), 4.57 (2 H, s, CH_2Ph), 4.23 (1 H, dd, J 5.4 and 4.0 Hz, 4-H), 4.01 (1 H, q, J 3.5 Hz, 5-H), 3.75 (1 H, dd, J 10.6 and 3.0 Hz, 5-CHH), 3.63 (1 H, dd, J 10.7 and 4.0 Hz, 5-CHH), 2.66 (3 H, d, J 4.6 Hz, MeNH).

(2R,3R,4S,5R)-2-(6-Amino-8-methylaminopurin-9-yl)-5-cyclohexylmethoxymethyltetrahydrofuran-3,4-diol (5). Synthesis was as described for **4**. LC—MS: m/z 393 [M + H]$^+$; t_R = 1.84 min; total run time 3.75 min. ^{1}H NMR: δ_H (DMSO-d_6) 7.91 (1 H, s, ArH), 6.48 (2 H, s, NH$_2$), 6.43 (1 H, q, J 4.4 Hz, MeNH), 5.79 (1 H, d, J 6.0 Hz, 2-H), 5.30 (1 H, br s, 3-OH), 5.15 (1 H, br s, 4-OH), 4.76 (1 H, t, J 5.7 Hz, 3-H), 4.19 (1 H, t, J 4.4 Hz, 4-H), 3.96 (1 H, q, J 3.7 Hz, 5-H), 3.66 (1 H, dd, J 10.8 and 2.9 Hz, 5-CHHO), 3.51 (1H, dd, J 10.8 and 4.13 Hz, 5-CHHO), 3.31 (1 H, dd, J 9.6 and 6.3 Hz, OCHHcycloalkyl), 3.20 (1 H, dd, J 9.5 and 7.2 Hz, OCHHcycloalkyl), 2.92 (3 H, d, J 4.6 Hz, MeNH), 1.50—1.71 (6 H, m, cycloalkyl), 1.10—1.20 (3 H, m, cycloalkyl), 0.82—0.92 (2 H, m, cycloalkyl).

(2R,3R,4S,5R)-2-(6-Amino-8-methylaminopurin-9-yl)-5-(pyridin-3-ylmethoxymethyl)tetrahydrofuran-3,4-diol (6). Synthesis was as described for **4**. LC—MS: m/z 388 [M + H]$^+$; t_R = 1.19 min; total run time 3.75 min. ^{1}H NMR: δ_H (DMSO-d_6) 8.56 (1 H, d,

J 1.7 Hz, pyridyl 2-H), 8.52 (1 H, dd, J 4.8 and 1.6 Hz, pyridyl 6-H), 7.90 (1 H, s, ArH), 7.70 (1 H, dt, J 7.9, 1.7, and 1.7 Hz, pyridyl 5-H), 7.38 (1 H, dd, 7.9 and 4.8 Hz, pyridyl 4-H), 6.47 (2 H, s, NH_2), 6.45 (1 H, q, J 4.6 Hz, MeNH), 5.79 (1 H, d, J 5.9 Hz, 2-H), 5.34 (1 H, br s, 3-OH), 5.19 (1 H, br s, 4-OH), 4.81 (1 H, t, J 5.6 Hz, 3-H), 4.60 (2 H, s, OCH_2Ar), 4.26 (1 H, t, J 4.5 Hz, 4-H), 4.01 (1 H, q, 4.1 Hz, 5-H), 3.78 (1 H, dd, J 10.7 and 3.1 Hz, 5-CHH), 3.65 (1 H, dd, J 10.7 and 4.3 Hz, 5-CHH), 2.69 (3 H, d, J 4.6 Hz, MeNH),

2-[(2R,3S,4R,5R)-5-(6-Amino-8-methylaminopurin-9-yl)-3,4-dihydroxytetrahydrofuran-2-ylmethoxy]acetamide (7). Synthesis was as described for **4**. LC—MS: m/z 354 $[M + H]^+$; t_R = 0.86 min; total run time 3.75 min. ^{1}H NMR: δ_H (DMSO-d_6) 7.90 (1 H, s, ArH), 7.28 (1 H, br s, CONHH) 7.22 (1 H, br s, CONHH), 6.58 (1 H, q, J 4.7 Hz, MeNH), 6.46 (2 H, s, NH_2), 5.75 (1 H, d, J 6.2 Hz, 2-H), 5.28 (2 H, br s, 3- and 4-OH), 4.90 (1 H, t, J 5.9 Hz, 3-H), 4.27 (1 H, dd, J 5.6 and 3.9 Hz, 4-H), 3.99 (1 H, q, J 3.9 Hz, 5-H), 3.87 [2 H, d, J 1.5 Hz, CH_2C(O)NH_2], 3.78 (1 H, dd, J 10.7 and 3.0 Hz, 5-CHH), 3.63 (1 H, dd, J 10.7 and 4.4 Hz, 5-CHH), 2.89 (3 H, d, J 4.5 Hz, MeNH).

(2R,3R,4S,5R)-2-{6-Amino-8-[(quinolin-2-ylmethyl)amino]purin-9-yl}-5-hydroxymethyltetrahydrofuran-3,4-diol (10). A suspension of (2R,3R,4S,5R)-2-(6-amino-8-bromopurin-9-yl)-5-hydroxymethyltetrahydrofuran-3,4-diol (8-bromoadenine-9-β-D-ribofuranoside) (**19**) (0.50 g, 1.45 mmol) and 3,4-dichlorobenzylamine (1.93 mL, 14.4 mmol) in ethanol (15 mL) was heated with microwaves in a sealed tube at 170 °C for 30 min.[28] The solvent was removed in vacuo. The resultant residue was dissolved in methanol—dichloromethane (1:4, 75 mL), and then PS-benzaldehyde (13.0 g, 13.0 mmol) was added. The suspension was stirred at room temperature overnight. The PS-benzaldehyde was removed by filtration and the solvent removed in vacuo from the filtrate. The resultant crude product was purified by silica gel (25 g) flash column chromatography [methanol—dichloromethane (5—10% gradient)] to afford the desired product **10** as a white solid (0.116 g, 0.26 mmol, 25%). LC—MS: m/z 424 $[M + H]^+$; t_R = 1.44 min; total run time 3.75 min. ^{1}H NMR: δ_H (DMSO-d_6) 8.32 (1 H, d, J 8.5 Hz, Ar-H), 7.93—7.99 (2 H, m, 2 × Ar-H), 7.91 (1 H, s, Ar-H), 7.75—7.77 (2 H, m, 2 × Ar-H), 7.54—7.59 (2 H, m, NHMe and Ar-H), 6.53 (2 H, s, NH_2), 6.00 (1 H, d, J 7.4 Hz, 2-H), 5.87 (1 H, dd, J 6.2 and 4.1 Hz, 5-CH$_2$OH), 5.36 (1 H, d, J 6.7 Hz, 3-OH), 5.19 (1 H, d, J 4.0 Hz, 4-OH), 4.80—4.81 (3 H, m, 3-H and CH_2Ar), 4.14—4.17 (1 H, m, 4-H), 4.02 (1 H, m, 5-H), 3.62—3.70 (2 H, m, 5-CH_2OH).

(3aR,4R,6R,6aR)-[6-(6-Amino-8-methylaminopurin-9-yl)-2,2-dimethyltetrahydrofuro[3,4-d][1,3]dioxol-4-yl]methanol (16). A suspension of **15**[26,33] (0.50 g, 1.3 mmol) in methylamine (33% in ethanol, 5 mL) was heated in a sealed tube with microwaves at 130 °C for 45 min. The solvent was then removed in vacuo. The residual crude product was purified by silica gel (50 g) flash chromatography, eluting with dichloromethane—methanol (95:5 to 90:10 gradient) to afford the desired product **16** as a white foam (0.40 g, 1.19 mmol, 91%). LC—MS: m/z 337 $[M + H]^+$; t_R = 1.46 min; total run time 3.75 min. ^{1}H NMR: δ_H (DMSO-d_6) 7.91 (1 H, s, Ar-H), 6.96 (1 H, q, J 4.4 Hz, MeNH), 6.59 (2 H, s, NH_2), 5.99 (1 H, d, J 3.6 Hz, 2-H), 5.49 (1 H, t, J 5.3 Hz, CH$_2$OH), 5.42 (1 H, m, 3-H), 4.97 (1 H, dd, J 2.8 and 3.5 Hz, 4-H), 4.15 (1 H, m, 5-H), 3.55 (2 H, m, CH_2OH), 2.88 (3 H, d, J 4.6 Hz, MeNH), 1.54 (3 H, S, MeMeC), 1.30 (3 H, s, MeMeC).

9-{(3aR,4R,6R,6aR)-6-Benzyloxymethyl-2,2-dimethyltetrahydrofuro[3,4-d][1,3]dioxol-4-yl}-N8-methyl-9H-purine-6,8-diamine (17a) and (3aR,4R,6R,6aR)-{6-[6-Amino-8-(benzylmethylamino)purin-9-yl]-2,2-dimethyltetrahydrofuro[3,4-d][1,3]dioxol-4-yl}methanol (18a). Cesium carbonate (0.156 g, 0.48 mmol) and benzyl chloride (0.033 mL, 0.28 mmol) were added sequentially to a solution of **16**[27] (0.080 g, 0.24 mmol) in DMF (5 mL). The mixture was stirred at room temperature for ~72 h. The solvent was removed in vacuo. Then the resulting residue was partitioned between ethyl acetate (20 mL) and water (10 mL). The organic

extract was dried (MgSO$_4$) and the solvent removed in vacuo. The resultant crude product was purified by silica gel (10 g) flash chromatography, eluting with dichloromethane—methanol (98:2 to 95:55 gradient) to afford the desired products **17a** and **18b** as a cream glass (0.044 g, 0.10 mmol, 42%). LC—MS: m/z 427 $[M + H]^+$; t_R = 2.04 and 2.13 min; total run time 3.75 min.

Protein Expression and Purification. Expression trials of the GST tagged, ATPase plasmid pRT860 was initiated in the *E. coli* BL21 DE3 strain. Expression was achieved overnight after induction with 0.6 mM IPTG and temperature reduction to 18 °C. The cells were subsequently harvested after 18 h of growth and yielded approximately 6 mg/mL protein. The cell paste was frozen immediately for later use or lysed using an Emulsiflex cell disrupter. Lysed cells were clarified for 1 h at 30 000 rpm. Cleared lysates were loaded onto a 5 mL glutathione *S*-transferase column. Pooled peak fractions were eluted with 50 mM Tris-HCl, pH 8, 100 mM NaCl, 1 mM DTT, and 10 mM glutathione. To achieve crystallizable material, the tagged protein was cleaved. A final polishing step using a HiLoad 16-60 SD200pg column eluted with 20 mM Tris-HCl, pH 7.5, 200 mM NaCl, and 1 mM DTT gave very pure material. The Grp78 protein included the residues 24—407. The Hsc70 protein included residues 5—381. Hsc70 and Bag-1 were prepared as previously described.[22]

Crystallization and Structure Determination. Very thin plates of apo Grp78 crystals were obtained from purified protein mixed with 0.1 M Tris buffer, pH 8.4—8.6, 20—25% Peg3350, 0.1—0.2 M Na, K tartrate, in hanging drop vapor diffusion experiments, carried out at 293 K. Because of merohedral twinning, single crystals had to be selected by initial X-ray diffraction examination. Crystallization of Hsc70/Bag-1 has been described in Sondermann et al.[6] Diffraction data were acquired on Rigaku RUH3 rotating anode X-ray source equipped with Raxis IV++ image plate detector (Hsc70/Bag-1/7) or at ESRF synchrotron beamline ID29 (Grp78 apo and complexes and ID23-1 (Hsc70/Bag-1/10). Data were processed with Rigaku/MSC's CrystalClear or HKL2000[34] software. Structures were solved by molecular replacement using the Hsc70 3fzf[22] structure as the starting model for Grp78 and different and/or missing fragments/side chains built in, and the structure was refined.

Grp78 ATPase domain (residues 24-407) crystallized in the monoclinic $P2_1$ space group with two independent molecules in the unit cell. Apo crystals of Grp78 were soaked in a DMSO solution of the ligands or in an aqueous solution of ATP or ADPnP at pH 7.5. Ligands were fitted into difference Fourier electron density maps and subsequently included in refinement. Model corrections and structure refinement were iteratively carried out with COOT[35] and Refmac[36] (as implemented in the CCP4i suite[37]). Structures of Hsc70/Bag-1 were solved as previously described.[22]

Surface Plasmon Resonance (SPR). SPR measurements were performed on BIAcore T100 instrument (BIAcore GE Healthcare), at 25 °C on series S NTA chips (certified) according to provider's protocols with 10 mM HEPES, pH 7.4, 150 mM NaCl, 500 μM EDTA, 0.05% Tween-20, and 1% DMSO as a running buffer. Histidine-tagged Grp78 was immobilized on the sensor surface; reference surfaces without immobilized Ni^{2+} served as controls for nonspecific binding and refractive index changes. Concentrations of inhibitors (0—200 μM) were typically injected over the sensor chip at 35 μL/min. Zero concentration samples were used as blanks. The sensor surface was regenerated between experiments by injections of 0.1 mg/mL trypsin and 50% DMSO. Data processing was performed using BIAevaluation 2.1 software (BIAcore GE Healthcare Bio-Sciences Corp.) by globally fitting the entire inhibitor concentration series data set to the steady state affinity model.

Isothermal Titration Calorimetry. ITC measurements were performed using an iTC200 instrument (Microcal, GE Healthcare), with 11 μM protein at 25 °C, 10 mM HEPES, pH 7.4, 150 mM NaCl, 500 μM EDTA, 5 mM monothioglycerol, 0.05% Tween-20, and 1% DMSO. All data were fitted to a one site model using the provided software.

■ ASSOCIATED CONTENT

ⓢ Supporting Information. Crystallographic and refinement data, sample ITC data, siRNA data and methods, model of Grp78/**14**, and sequence alignment of protein isoforms. This material is available free of charge via the Internet at http://pubs.acs.org.

Accession Codes

■ AUTHOR INFORMATION

Corresponding Author

*Phone: +44 (0)1223 895555. Fax: +44 (0)1223 895556. E-mail: a.macias@vernalis.com.

■ ACKNOWLEDGMENT

■ ABBREVIATIONS USED

ADP, adenosine 5′-diphosphate; ADPnP, 5′-adenylyl β,γ-imidodiphosphate; ATP, adenosine 5′-triphosphate; Bag-1, BCL-2-associated athanolgene 1; BiP, immunoglobulin heavy-binding protein; Cα, α carbon; DMSO, dimethylsulfoxide; EGCG, (−)-epigallocatechin gallate; ER, endoplasmic reticulum; FP, fluorescence polarization; Grp78, 78 kDa glucose regulated protein; ΔH, enthalpy change; ΔS, entropy change; K_D, dissociative constant; k_d, off-rate; HCT116, human colon tumor 116; HEPES, 4-(2-hydroxyethyl)-1-piperazineethanesulfonic acid; HSC70, 70 kDa heat shock cognate protein; HSP, heat shock protein; HSP70, 70 kDa heat shock protein; ITC, isothermal titration calorimetry; rmsd, root-mean-square deviation; SBD, substrate binding domain; siRNA, short interfering ribonucleic acid; SPR, surface plasmon resonance; Tris, (hydroxymethyl)aminomethane; UPR, unfolded protein response; VST, versipelostatin

■ REFERENCES

(1) Mayer, M. P.; Bukau, B. Hsp70 chaperones: cellular functions and molecular mechanism. *Cell. Mol. Life Sci.* **2005**, *62*, 670–684.

(2) Bukau, B.; Weissman, J.; Horwich, A. Molecular chaperones and protein quality control. *Cell* **2006**, *125*, 443–451.

(3) Jiang, J.; Prasad, K.; Lafer, E. M.; Sousa, R. Structural basis of interdomain communication in the Hsc70 chaperone. *Mol. Cell* **2005**, *20*, 513–524.

(4) Vogel, M.; Bukau, B.; Mayer, M. P. Allosteric regulation of Hsp70 chaperones by a proline switch. *Mol. Cell* **2006**, *21*, 359–367.

(5) Amor-Mahjoub, M.; Gomez-Vrielyunck, N.; Suppini, J. P.; Fouchaq, B.; Benarouj, N.; Ladjimi, M. Involvement of the interdomain hydrophobic linker and the C-terminal helices in self-association of the molecular chaperone HSC70. *Arch. Inst. Pasteur Tunis* **2006**, *83*, 53–62.

(6) Sondermann, H.; Scheufler, C.; Schneider, C.; Hohfeld, J.; Hartl, F. U.; Moarefi, I. Structure of a Bag/Hsc70 complex: convergent functional evolution of Hsp70 nucleotide exchange factors. *Science* **2001**, *291*, 1553–1557.

(7) Haas, I. G. BiP (GRP78), an essential hsp70 resident protein in the endoplasmic reticulum. *Experientia* **1994**, *S0*, 1012–1020.

(8) Lee, A. S. The ER chaperone and signaling regulator GRP78/BiP as a monitor of endoplasmic reticulum stress. *Methods* **2005**, *3S*, 373–381.

(9) Dong, D.; Ni, M.; Li, J.; Xiong, S.; Ye, W.; Virrey, J. J.; Mao, C.; Ye, R.; Wang, M.; Pen, L.; Dubeau, L.; Groshen, S.; Hofman, F. M.; Lee, A. S. Critical role of the stress chaperone GRP78/BiP in tumor proliferation, survival, and tumor angiogenesis in transgene-induced mammary tumor development. *Cancer Res.* **2008**, *68*, 498–505.

(10) Li, J.; Lee, A. S. Stress induction of GRP78/BiP and its role in cancer. *Curr. Mol. Med.* **2006**, *6*, 45–54.

(11) Misra, U. K.; Gonzalez-Gronow, M.; Gawdi, G.; Pizzo, S. V. The role of MTJ-1 in cell surface translocation of GRP78, a receptor for alpha 2-macroglobulin-dependent signaling. *J. Immunol.* **2005**, *174*, 2092–2097.

(12) Delpino, A.; Castelli, M. The 78 kDa glucose-regulated protein (GRP78/BIP) is expressed on the cell membrane, is released into cell culture medium and is also present in human peripheral circulation. *Biosci. Rep.* **2002**, *22*, 407–420.

(13) Kelber, J. A.; Panopoulos, A. D.; Shani, G.; Booker, E. C.; Belmonte, J. C.; Vale, W. W.; Gray, P. C. Blockade of Cripto binding to cell surface GRP78 inhibits oncogenic Cripto signaling via MAPK/PI3K and Smad2/3 pathways. *Oncogene* **2009**, *28*, 2324–2336.

(14) Misra, U. K.; Deedwania, R.; Pizzo, S. V. Activation and cross-talk between Akt, NF-kappaB, and unfolded protein response signaling in 1-LN prostate cancer cells consequent to ligation of cell surface-associated GRP78. *J. Biol. Chem.* **2006**, *281*, 13694–13707.

(15) Ranganathan, A. C.; Zhang, L.; Adam, A. P.; Aguirre-Ghiso, J. A. Functional coupling of p38-induced up-regulation of BiP and activation of RNA-dependent protein kinase-like endoplasmic reticulum kinase to drug resistance of dormant carcinoma cells. *Cancer Res.* **2006**, *66*, 1702–1711.

(16) Reddy, R. K.; Mao, C.; Baumeister, P.; Austin, R. C.; Kaufman, R. J.; Lee, A. S. Endoplasmic reticulum chaperone protein GRP78 protects cells from apoptosis induced by topoisomerase inhibitors: role of ATP binding site in suppression of caspase-7 activation. *J. Biol. Chem.* **2003**, *278*, 20915–20924.

(17) Lee, A. S. GRP78 induction in cancer: therapeutic and prognostic implications. *Cancer Res.* **2007**, *67*, 3496–3499.

(18) Park, H. R.; Furihata, K.; Hayakawa, Y.; Shin-Ya, K. Versipelostatin, a novel GRP78/Bip molecular chaperone down-regulator of microbial origin. *Tetrahedron Lett.* **2010**, *43*, 6941–6945.

(19) Yoneda, Y.; Steiniger, S. C.; Capkova, K.; Mee, J. M.; Liu, Y.; Kaufmann, G. F.; Janda, K. D. A cell-penetrating peptidic GRP78 ligand for tumor cell-specific prodrug therapy. *Bioorg. Med. Chem. Lett.* **2008**, *18*, 1632–1636.

(20) Kim, Y.; Lillo, A. M.; Steiniger, S. C.; Liu, Y.; Ballatore, C.; Anichini, A.; Mortarini, R.; Kaufmann, G. F.; Zhou, B.; Felding-Habermann, B.; Janda, K. D. Targeting heat shock proteins on cancer cells: selection, characterization, and cell-penetrating properties of a peptidic GRP78 ligand. *Biochemistry* **2006**, *45*, 9434–9444.

(21) Misra, U. K.; Mowery, Y.; Kaczowka, S.; Pizzo, S. V. Ligation of cancer cell surface GRP78 with antibodies directed against its COOH-terminal domain up-regulates p53 activity and promotes apoptosis. *Mol. Cancer Ther* **2009**, *8*, 1350–1362.

(22) Williamson, D. S.; Borgognoni, J.; Clay, A.; Daniels, Z.; Dokurno, P.; Drysdale, M. J.; Foloppe, N.; Francis, G. L.; Graham, C. J.; Howes, R.; Macias, A. T.; Murray, J. B.; Parsons, R.; Shaw, T.; Surgenor, A. E.; Terry, L.; Wang, Y.; Wood, M.; Massey, A. J. Novel adenosine-derived inhibitors of 70 kDa heat shock protein, discovered through structure-based design. *J. Med. Chem.* **2009**, *52*, 1510–1513.

(23) Massey, A. J.; Williamson, D. S.; Browne, H.; Murray, J. B.; Dokurno, P.; Shaw, T.; Macias, A. T.; Daniels, Z.; Geoffroy, S.; Dopson, M.; Lavan, P.; Matassova, N.; Francis, G. L.; Graham, C. J.; Parsons, R.; Wang, Y.; Padfield, A.; Comer, M.; Drysdale, M. J.; Wood, M. A novel, small molecule inhibitor of Hsc70/Hsp70 potentiates Hsp90 inhibitor induced apoptosis in HCT116 colon carcinoma cells. *Cancer Chemother. Pharmacol.* **2010**, *66*, 535–545.

(24) Holmes, R. E.; Robins, R. K. Purine Nucleosides. IX. The synthesis of 9-beta-D-ribofuranosyl uric acid and other related 8-substituted purine ribonucleosides. *J. Am. Chem. Soc.* **1965**, *87*, 1772–1776.

(25) Long, R. A.; Robinds, R. K.; Townsend, L. B. Purine nucleosides. XV. The synthesis of 8-amino and 8-substituted aminopurine nucleosides. *J. Org. Chem.* **1967**, *32*, 2751–2756.

(26) Ikehara, M.; Tada, H.; Muneyama, K.; Kaneko, M. Synthesis of purine cyclonucleoside having an 8,2′-O-anhydro linkage. *J. Am. Chem. Soc.* **1966**, *88*, 3165–3167.

(27) Sasaki, T.; Minamoto, K.; Fujiki, Y. Systematic synthesis of purine 8,5′-imino and substituted imino cyclonucleosides. *Chem. Lett.* **1983**, *7*, 1017–1020.

(28) Chattopadhyaya, J. B.; Reese, C. B. Reaction between 8-bromoadenosine and amines. Chemistry of 8-hydrazinoadenosine. *Synthesis* **1977**, *10*, 725–726.

(29) Huang, X. Fluorescence polarization competition assay: the range of resolvable inhibitor potency is limited by the affinity of the fluorescent ligand. *J. Biomol. Screening* **2003**, *8*, 34–38.

(30) Cer, R. Z.; Mudunuri, U.; Stephens, R.; Lebeda, F. J. IC_{50}-to-K_i: a Web-based tool for converting IC_{50} to K_i values for inhibitors of enzyme activity and ligand binding. *Nucleic Acids Res.* **2009**, *37*, W441–W445.

(31) Wisniewska, M.; Karlberg, T.; Lehtio, L.; Johansson, I.; Kotenyova, T.; Moche, M.; Schuler, H. Crystal structures of the ATPase domains of four human Hsp70 isoforms: HSPA1L/Hsp70-hom, HSPA2/Hsp70-2, HSPA6/Hsp70B′, and HSPA5/BiP/GRP78. *PLoS One* **2010**, *5*, No. e8625.

(32) Altschul, S. F.; Madden, T. L.; Schaffer, A. A.; Zhang, J.; Zhang, Z.; Miller, W.; Lipman, D. J. Gapped BLAST and PSI-BLAST: a new generation of protein database search programs. *Nucleic Acids Res.* **1997**, *25*, 3389–3402.

(33) Schmitt, L.; Tampe, R. ATP-lipids-protein anchor and energy source in two dimensions. *J. Am. Chem. Soc.* **1996**, *118*, 5532–5543.

(34) Otwinowski, Z.; Minor, W. Processing of X-ray diffraction data collected in oscillation mode. *Methods Enzymol.* **1997**, *276*, 307–326.

(35) Emsley, P.; Cowtan, K. Coot: model-building tools for molecular graphics. *Acta Crystallogr., Sect. D: Biol. Crystallogr.* **2004**, *60*, 2126–2132.

(36) Murshudov, G. N.; Vagin, A. A.; Dodson, E. J. Refinement of macromolecular structures by the maximum-likelihood method. *Acta Crystallogr., Sect. D: Biol. Crystallogr.* **1997**, *53*, 240–255.

(37) Potterton, E.; Briggs, P.; Turkenburg, M.; Dodson, E. A graphical user interface to the CCP4 program suite. *Acta Crystallogr., Sect. D: Biol. Crystallogr.* **2003**, *59*, 1131–1137.